Low temperature transferring of anodized TiO_2 nanotube-array onto a flexible substrate for dye-sensitized solar cells

Shu Zhu,[1] Xiaolin Liu,[1] Jia Lin,[2] and Xianfeng Chen[1,2*]

[1]*State Key Laboratory of Advanced Optical Communication Systems and Networks, Department of Physics and Astronomy, Shanghai Jiao Tong University, 800 Dongchuan Road, Shanghai 200240, China*
[2]*Department of Physics, Shanghai University of Electric Power, Shanghai 200090, China*
[*]*xfchen@sjtu.edu.cn*

Abstract: In this paper, free-standing TiO_2 nanotube membranes are transferred onto ITO/PET substrates using binder-free TiO_2 pastes. Followed by laser sintering, the electrical contacts between the TiO_2 nanotube membrane, nanoparticles and substrate can be efficiently promoted, which prevents from damaging to the plastic conductive substrate. The efficiency of 4.65% is achieved without traditional high temperature sintering and mechanical compression, which shows great potential application in TiO_2 nanotube based flexible dye-sensitized solar cells (DSSCs).

OCIS codes: (160.0160) Materials; (160.4236) Nanomaterials.

References and links

1. D. L. Klass, *Biomass for Renewable Energy, Fuels, and Chemicals* (Academic Press, 1998).
2. I. Dincer, "Renewable energy and sustainable development: a crucial review," Renew. Sustain. Energy Rev. **4**(2), 157–175 (2000).
3. M. H. Huesemann, "The limits of technological solutions to sustainable development," Clean Technol. Envir. **5**, 21–34 (2003).
4. M. Grätzel, "Solar energy conversion by dye-sensitized photovoltaic cells," Inorg. Chem. **44**(20), 6841–6851 (2005).
5. M. Grätzel, "Recent advances in sensitized mesoscopic solar cells," Acc. Chem. Res. **42**(11), 1788–1798 (2009).
6. L. Han, A. Islam, H. Chen, C. Malapaka, B. Chiranjeevi, S. Zhang, X. Yang, and M. Yanagida, "High-efficiency dye-sensitized solar cell with a novel co-adsorbent," Energy Environ. Sci. **5**(3), 6057–6060 (2012).
7. J. Burschka, N. Pellet, S.-J. Moon, R. Humphry-Baker, P. Gao, M. K. Nazeeruddin, and M. Grätzel, "Sequential deposition as a route to high-performance perovskite-sensitized solar cells," Nature **499**(7458), 316–319 (2013).
8. C. Longo, J. Freitas, and M.-A. De Paoli, "Performance and stability of TiO_2 dye solar cells assembled with flexible electrodes and a polymer electrolyte," J. Photochem. Photobiol. Chem. **159**(1), 33–39 (2003).
9. S. Ito, N. L. Ha, G. Rothenberger, P. Liska, P. Comte, S. M. Zakeeruddin, P. Péchy, M. K. Nazeeruddin, and M. Grätzel, "High-efficiency (7.2%) flexible dye-sensitized solar cells with Ti-metal substrate for nanocrystalline-TiO_2 photoanode," Chem. Commun. (Camb.) **38**(38), 4004–4006 (2006).
10. M. G. Kang, N.-G. Park, K. S. Ryu, S. H. Chang, and K.-J. Kim, "A 4.2% efficient flexible dye-sensitized TiO_2 solar cells using stainless steel substrate," Sol. Energy Mater. Sol. Cells **90**(5), 574–581 (2006).
11. Y. Wang, J. Wu, Z. Lan, Y. Xiao, Q. Li, F. Peng, J. Lin, and M. Huang, "Preparation of porous nanoparticle TiO_2 films for flexible dye-sensitized solar cells," Chin. Sci. Bull. **56**(24), 2649–2653 (2011).
12. J.-C. Tinguely, R. Solarska, A. Braun, and T. Graule, "Low-temperature roll-to-roll coating procedure of dye-sensitized solar cell photoelectrodes on flexible polymer-based substrates," Semicond. Sci. Technol. **26**(4), 045007 (2011).
13. M. Dürr, A. Schmid, M. Obermaier, S. Rosselli, A. Yasuda, and G. Nelles, "Low-temperature fabrication of dye-sensitized solar cells by transfer of composite porous layers," Nat. Mater. **4**(8), 607–611 (2005).
14. S.-S. Kim, J.-H. Yum, and Y.-E. Sung, "Flexible dye-sensitized solar cells using ZnO coated TiO_2 nanoparticles," J. Photochem. Photobiol. Chem. **171**(3), 269–273 (2005).
15. N. G. Park, K. M. Kim, M. G. Kang, K. Ryu, S. Chang, and Y. J. Shin, "Chemical sintering of nanoparticles: a methodology for low-temperature fabrication of dye-sensitized TiO_2 films," Adv. Mater. **17**(19), 2349–2353 (2005).

#249353 Received 2 Sep 2015; revised 13 Oct 2015; accepted 30 Oct 2015; published 4 Nov 2015

16. W. Tan, X. Yin, X. Zhou, J. Zhang, X. Xiao, and Y. Lin, "Electrophoretic deposition of nanocrystalline TiO_2 films on Ti substrates for use in flexible dye-sensitized solar cells," Electrochim. Acta **54**(19), 4467–4472 (2009).
17. T. N. Murakami, Y. Kijitori, N. Kawashima, and T. Miyasaka, "Low temperature preparation of mesoporous TiO_2 films for efficient dye-sensitized photoelectrode by chemical vapor deposition combined with UV light irradiation," J. Photochem. Photobiol. Chem. **164**(1-3), 187–191 (2004).
18. Y.-Y. Kuo and C.-H. Chien, "Sinter-free transferring of anodized TiO_2 nanotube-array onto a flexible and transparent sheet for dye-sensitized solar cells," Electrochim. Acta **91**, 337–343 (2013).
19. M. G. Kang, N.-G. Park, K. S. Ryu, S. H. Chang, and K.-J. Kim, "A 4.2% efficient flexible dye-sensitized TiO_2 solar cells using stainless steel substrate," Sol. Energy Mater. Sol. Cells **90**(5), 574–581 (2006).
20. B. O'Regan and M. Grätzel, "A low-cost high-efficiency solar cell based on dye-sensitized colloidal TiO_2 thin film," Nature **353**(6346), 737–740 (1991).
21. X. Luan, D. Guan, and Y. Wang, "Facile synthesis and morphology control of bamboo-type TiO_2 nanotube arrays for high-efficiency dye-sensitized solar cells," J. Phys. Chem. C **116**(27), 14257–14263 (2012).
22. W. Guo, X. Xue, S. Wang, C. Lin, and Z. L. Wang, "An integrated power pack of dye-sensitized solar cell and Li battery based on double-sided TiO_2 nanotube arrays," Nano Lett. **12**(5), 2520–2523 (2012).
23. G. K. Mor, K. Shankar, M. Paulose, O. K. Varghese, and C. A. Grimes, "Use of highly-ordered TiO_2 nanotube arrays in dye-sensitized solar cells," Nano Lett. **6**(2), 215–218 (2006).
24. P. Roy, D. Kim, K. Lee, E. Spiecker, and P. Schmuki, "TiO_2 nanotubes and their application in dye-sensitized solar cells," Nanoscale **2**(1), 45–59 (2010).
25. D. Kuang, J. Brillet, P. Chen, M. Takata, S. Uchida, H. Miura, K. Sumioka, S. M. Zakeeruddin, and M. Grätzel, "Application of highly ordered TiO_2 nanotube arrays in flexible dye-sensitized solar cells," ACS Nano **2**(6), 1113–1116 (2008).
26. K. Shankar, G. K. Mor, H. E. Prakasam, S. Yoriya, M. Paulose, O. K. Varghese, and C. A. Grimes, "Highly-ordered TiO_2 nanotube arrays up to 220 μm in length: use in water photoelectrolysis and dye-sensitized solar cells," Nanotechnology **18**(6), 065707 (2007).
27. H.-P. Jen, M.-H. Lin, L.-L. Li, H.-P. Wu, W.-K. Huang, P.-J. Cheng, and E. W.-G. Diau, "High-performance large-scale flexible dye-sensitized solar cells based on anodic TiO2 nanotube arrays," ACS Appl. Mater. Inter. **5**, 10104 (2013).
28. P.-T. Hsiao, Y.-J. Liou, and H. Teng, "Electron transport patterns in TiO_2 nanotube arrays based dye-sensitized solar cells under frontside and backside illuminations," J. Phys. Chem. C **115**(30), 15018–15024 (2011).
29. J. Lin, J. Chen, and X. Chen, "Facile fabrication of free-standing TiO_2 nanotube membranes with both ends open via self-detaching anodization," Electrochem. Commun. **12**(8), 1062–1065 (2010).
30. J. H. Park, T. W. Lee, and M. G. Kang, "Growth, detachment and transfer of highly-ordered TiO_2 nanotube arrays: use in dye-sensitized solar cells," Chem. Commun. (Camb.) **25**(25), 2867–2869 (2008).
31. A. Lamberti, A. Sacco, S. Bianco, D. Manfredi, M. Armandi, M. Quaglio, E. Tresso, and C. F. Pirri, "An easy approach for the fabrication of TiO_2 nanotube-based transparent photoanodes for dye-sensitized solar cells," Sol. Energy **95**, 90–98 (2013).
32. J. Lin, J. Chen, and X. Chen, "High-efficiency dye-sensitized solar cells based on robust and both-end-open TiO_2 nanotube membranes," Nanoscale Res. Lett. **6**(1), 475 (2011).
33. L. Ming, H. Yang, W. Zhang, X. Zeng, D. Xiong, Z. Xu, H. Wang, W. Chen, X. Xu, M. Wang, J. Duan, Y.-B. Cheng, J. Zhang, Q. Bao, Z. Wei, and S. Yang, "Selective laser sintering of TiO_2 nanoparticle film on plastic conductive substrate for highly efficient flexible dye-sensitized solar cell application," J. Mater. Chem. A Mater. Energy Sustain. **2**(13), 4566–4573 (2014).

1. Introduction

With the development of science and technology, there is a growing need for energy consumption worldwide. To date, fossil fuels offer majority energy in the planet and have been excessively exploited [1]. In order to realize sustainable development while maintaining the environment from pollution, recycling and renewable energy have attracted much attention in recent studies [2, 3]. Dye sensitized solar cell (DSSC) is one of the underlying alternative owing to its good solar energy conversion efficiency with convenient fabrication processes [4–7]. In addition, flexible DSSCs have been widely researched since their unique properties such as portability, light weight and flexibility [8, 9]. Flexible DSSCs are usually fabricated on the limber materials. Contrary to traditional solar cells which require high temperature sintering to enhance the charge collection efficiency of the photoanode, flexible DSSCs can only be sintered in a relatively low temperature due to the restriction of limber materials [10–12]. Although a variety of methods have been employed toward the enhancement of energy conversion efficiency in DSSCs [13–18], some critical techniques such as poor heat resistance and fatigue of the flexible substrate remain for further improvement [19].

#249353 Received 2 Sep 2015; revised 13 Oct 2015; accepted 30 Oct 2015; published 4 Nov 2015

O'Regan and Grätzel first reported the DSSCs with disordered TiO_2 anatase nanoparticle films on transparent conducting oxide glass as photoanodes in 1991. The photoelectric conversion efficiency of the cells was 7.12% [20]. However, the losses in nanoparticulate DSSCs were large due to the high recombination of carries in TiO_2 nanoparticle network. In comparison to TiO_2 nanoparticles (TNP), TiO_2 nanotube (TNT) arrays with highly ordered structures provide a large internal surface and in the meanwhile introduce a free electron traveling path to reduce carrier recombination possibilities [21–26]. By applying the as-anodized TNT arrays as the photoelectrode, a flexible DSSC can be made because the as-anodized TNT arrays were developed on a bendy titanium foil [25, 27]. However, in such a device, the DSSC need to be illuminated backside, which is less favorable for DSSCs [28].

Recently, a self-detaching technique has been introduced for the synthesis of free-standing open-ended anodic nanotube membranes [29–31]. The achieved membranes can work as the front-side incident DSSCs when transferred to transparent substrates [32]. In this work, we successfully fabricated robust anodes via membrane transfer and laser sintering [33]. The free-standing membranes can be pre-annealed, and thus the high crystallinity will be ensured during the subsequent low-temperature treatment. Furthermore, the free-standing TNT membrane is transferred to plastic substrate using binder-free TiO_2 pastes and laser sintering. Both the procedures avoided the damage to the flexible substrate. The ability to fabricate these anodes of low temperature is of great necessity towards the exploitation of flexible DSSCs.

2. Experimental section

Preparation of TNT membranes

The TiO_2 nanotubes were fabricated by a previously developed potentiostatic anodization method, which leads to highly ordered nanotubes. In the experiment, the Ti foils play as the working electrode and Pt foils play as the counter electrode. Samples was processed in the electrolyte which consists of ethylene glycol + 3 vol% deionized water + 0.5 wt% ammonium fluoride (NH_4F). The working voltage of the three step anodization was set at 60 V using a computer controlled source meter. The anodization process includes three steps. First, the Ti substrate was pretreated by electrochemical method for 1 h at room temperature. Then we peeled off the TiO_2 layer to expose the substrate using ultrasonic machine. Thereafter the Ti was subjected the anodization for 1 h at room temperature again. Next the treated oxide layers experienced thermal treatment at 450 °C. Finally, the crystallized TNT membrane was detached via the third-step anodization at the temperature of 30 °C until the membrance and Ti substrate were separated.

DSSC assembly

2 g TiO_2 nanoparticles (TNPs) (P25, Degussa) were mixed with 10 ml 3.2 vol% acetic acid solution and 5 ml 10 M ammonia solution. The TiO_2 nanoparticle was spin-coated onto the substrate followed by the transferring of the TNT membranes on the substrate. Afterwards, the samples were treated by laser sintering. In the experiment, the focus point of the laser beam (center wavelength 1064 nm, laser power 2.5 W) was set 1 mm in front of the sample. The sample was put on a three dimensional translation stage as shown in Fig. 1(a). The sample was irradiated as the scanning speed of about 1 mm/s. The spot size of the laser beam was around 200 μm. And only 10 minutes are required to finish a size of 5*5 mm^2 pattern sintering. Figure 1(b) shows the scanning trace detailedly.

For comparison, three kinds of anodes for flexible DSSCs were prepared. The first is a photoanode composed of free-standing TNT membrane transferred onto PET substrate with ammonia added slurry as paste. Then it would be suffered with laser sintering (A-TiO_2 paste-LS). The second is a photoanode made up of free-standing TNT membrane transferred onto PET substrate with no ammonia added slurry as paste. Then it also would be suffered laser

#249353 Received 2 Sep 2015; revised 13 Oct 2015; accepted 30 Oct 2015; published 4 Nov 2015

sintering (NA-TiO_2 paste-LS). The last is a photoanode made of TNT membrane with no ammonia added slurry as paste. But it would be annealed in traditional furnace at the temperature of 100 °C (NA-TiO_2 paste-100 °C).

At last, the photoanodes were sensitized with the N719 dye (3×10^{-4} M in a 1:1 (*v/v*) acetonitrile and tert-butylalcohol solution) for 3 days. The Pt coated counter electrodes were fabricated by dipping H_2PtCl_6 isopropanol solution on FTO glass and thermally treated at 420 °C for 30 min. The photoanode and the counter electrode were separated by a 25-μm-thick spacer and the interspace was filled with DMPII/LiI/I_2/TBP/GuSCN in 3-methoxypropionitrile, a liquid electrolyte.

Measurements

The morphology of the free-standing TNT membrane was characterized using field-emission scanning electron microscopy (SEM, NOVA NanoSEM 230, FEI). The crystalline phase was collected by X-ray diffraction (XRD, Bruker D8 Advance, Germany). The current density-voltage (*J-V*) curves were measured under standard solar illumination (AM 1.5G, 100 mW cm^{-2}) by using an solar simulator (Model 91160, Newport-Oriel Instruments, USA) and the data were recorded by the 2400 sourcemeter (Keithley, USA).

3. Results and discussion

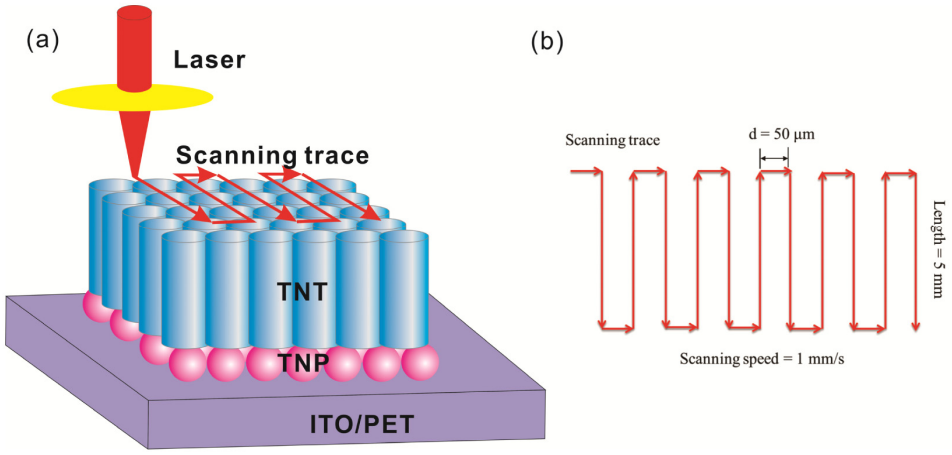

Fig. 1. (a) Schematic diagram of laser sintering process. Laser is focused by a convex lens and the red arrows represent the laser sintering scanning path. In the experiment, the focus of the laser was set 1 mm over the TNT membranes, with the ~200 μm diameter circular spot on the surface. (b) The scanning trace of laser. The scanning speed was set at 1mm/s.

Free-standing membranes are prepared with self-detaching method. As these TNT membranes have already been annealed at 450 °C after the second step anodization, the performance in charge transport remains the same, and no high temperature post-treatment is further needed.

Laser sintering employs a diode pump solid state laser to sinter the photoanode. Laser energy will be absorbed mostly by TNT membrane and TiO_2 paste [33]. In this way, the inter-nanoparticle connection will increase, which results in more fluent electron transfer path and less electron transfer resistance. Furthermore, the setting of the laser power, focal length and spot size are ensured to make the laser energy only be absorbed by TNT membrane and TiO_2 paste. Therefore, the plastic substrate can remain undamaged.

#249353 Received 2 Sep 2015; revised 13 Oct 2015; accepted 30 Oct 2015; published 4 Nov 2015

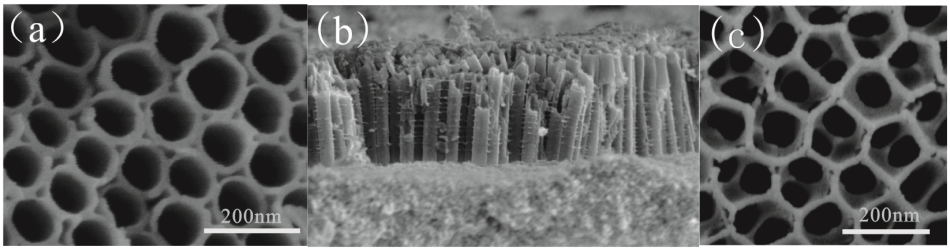

Fig. 2. SEM images showing free-standing nanotube layers. (a) The top view of the nanotube. (b) The cross section of nanotube and nanoparticles. (c) The top view of the nanotube after laser sintering.

Figure 2 shows the SEM picture of free-standing TNT membranes. The top view of the membrane is shown in Fig. 2(a). The diameter of pore is around 100 nm, which can be precisely tailored by employing different anodization parameters. Figure 2(b) shows the cross section of TNT membrane with a tube length of 19 μm and the TNPs which were used to adhere the membrane to the substrate. Figure 2(c) presents the top view of the nanotube after laser sintering. Although some damage can be observed at the surface of the nanotube, the whole tubular morphology is kept well.

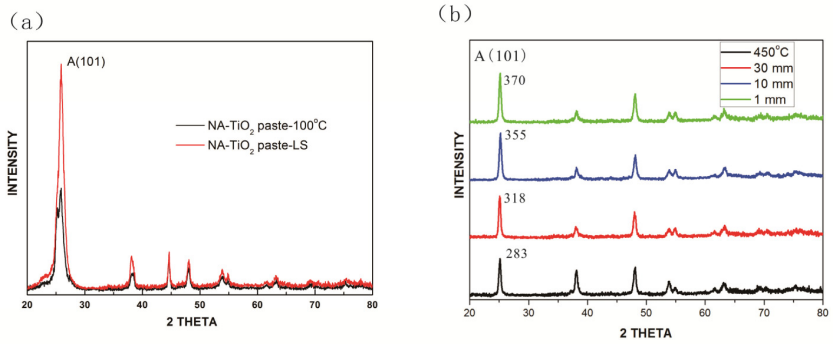

Fig. 3. (a) XRD patterns of sample with laser sintering and sample with 100 °C annealing in traditional furnace. (b) XRD patterns of sample with 450 °C in traditional furnace and samples with laser sintering at different position to the focus of laser beam from 1 to 30 millimeters.

We turned to XRD patterns of the photoanode based on NA-TiO_2 paste-LS and NA-TiO_2 paste-100 °C to characterize the laser sintering effect on the TiO_2 film. The results are shown in Fig. 3(a). The crystallization behavior of photoanode which is suffered laser sintering is much better than that of photoanode subjected to conventional 100 °C annealing. The enhanced crystallinity that led to the reduction of defects helps the improvement of the efficiency of the device, which would lead to the higher photoelectric conversion efficiency of DSSC based on NA-TiO_2 paste-LS compared with that based on NA-TiO_2 paste-100 °C. As we can see from Fig. 3(b), the effect of laser sintering was comparable to the 450 °C annealing in traditional furnace. The peak value of 101 respectively is also presented in Fig. 3(b). In addition, the effect of the samples at different position to the focus of laser beam from 1 to 30 had no obvious change. So, we could infer that the laser sintering was not only fast but also insensitive with the sintering condition.

#249353 Received 2 Sep 2015; revised 13 Oct 2015; accepted 30 Oct 2015; published 4 Nov 2015

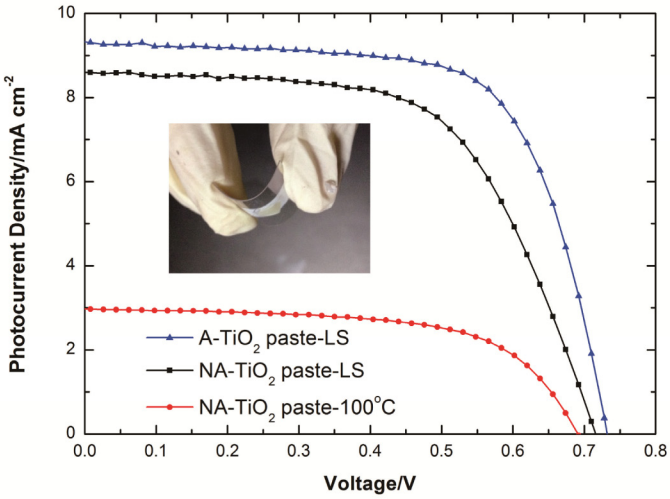

Fig. 4. J-V curves of solar cells based on A-TiO2 paste-LS, NA-TiO2 paste-LS and NA-TiO2 paste-100 °C. The inset present the picture of the free-standing membrane attached with PET substrate.

Table 1. The values of Jsc, Voc, FF, and η for the three types of DSSCs.

Photoanode	J_{sc} (mA/cm^2)	V_{oc} (V)	*FF*	η (%)
A-TiO$_2$ paste-LS	9.35	0.73	0.68	4.65
NA-TiO$_2$ paste-LS	8.66	0.71	0.61	3.75
NA-TiO$_2$ paste-100°C	2.99	0.67	0.65	1.35

The photocurrent-voltage (*J-V*) properties of DSSCs based on A-TiO_2 paste-LS and NA-TiO_2 paste-LS as well as NA-TiO_2 paste-100 °C are shown in Fig. 4 and Table 1. The NA-TiO_2 paste-100 °C -based DSSCs showed an efficiency (η) of 1.35% accompanied with a short-circuit photocurrent density (J_{sc}) of 2.99 mA/cm^2, open circuit voltage (V_{oc}) of 0.67 V, fill factor (*FF*) of 0.65. The NA-TiO_2 paste-LS-based DSSCs showed improved performance, with J_{sc} of 8.66 mA/cm^2, V_{oc} of 0.71V, *FF* of 0.61 and η of 3.75%. Efficiency increased by 178% compared to NA-TiO_2 paste-100 °C-based DSSC. The significant efficiency improvement is mainly due to the enhancement of inter-nanoparticle connection, which is caused by laser sintering. On the contrary, the paste of TNPs must be subjected to above 400 °C annealing in order to burn out the organic substances and then the electrical interconnect could be enhanced.

With A-TiO_2 paste-LS as the photoanode, J_{sc} of the DSSCs increased to 9.35 mA/cm^2, with V_{oc} of 0.73 V, *FF* of 0.68, and η of 4.65%. Efficiency increased by 24.1% compared to NA-TiO_2 paste-LS-based DSSC. The higher efficiency of A-TiO_2 paste-LS-based DSSCs was likely to be attributed to the addition of the ammonia which increased the viscosity of the TiO_2 colloid solution. The viscosity of the two kinds of paste was tested by bohlin CVO which was found that TiO_2 colloid solution with ammonia added was twice as much as the one without ammonia added. They were $1.97*10^3$ cP and $0.87*10^3$ cP respectively. (1cP = 1 mP s^{-1}) Therefor the interconnection among particles was enhanced and film resistance was decreased, enabling fast charge transport. Meanwhile the increased TiO_2-loading for film of the same thickness, led to increased total surface area of TiO_2 and hence a higher dye-loading. For the 19-μm-thick film, the TiO_2 loadings were 0.5195 mg·cm^{-2} and 0.3152 mg·cm^{-2} for with and without the addition of the ammonia. Compared with Jen's work [27], which developed high-performance large-scale flexible DSSCs based on anodic TiO_2 nanotube

#249353 Received 2 Sep 2015; revised 13 Oct 2015; accepted 30 Oct 2015; published 4 Nov 2015

arrays of about 35 μm length, our efficiency was a little lower than theirs, which may due to the shorter length of the nanotube. The inset of Fig. 4 presents the picture of the free-standing membrane attached with ITO/PET flexible substrate, which shows the flexibility is very good.

4. Conclusion

In conclusion, we successfully demonstrate the application of pre-annealed TiO_2 nanotube membranes as the photoanode materials and the laser sintering technique employing low-power and near-infrared diode pump solid state laser to adhere the membranes with conductive plastic substrates for flexible DSSC applications with good performance. This approach overcomes the high temperature limit of the flexible substrates. By using pre-annealed membranes, the crystallinity of photoanodes can be improved. The addition of ammonia to the TiO_2 nanoparticles (P25) slurry changes the flocculation of nanoparticles, thereby increasing the viscosity of the slurry. Furthermore, by laser sintering, the solvents present in the paste which links the TiO_2 nanotube membranes and flexible substrate can be removed. By applying these methods to DSSCs, the efficiency of the DSSCs can be greatly enhanced from 1.35% to 4.65%.

Acknowledgments

The work was supported by the National Natural Science Foundation of China (NSFC) (Grant No. 61125503, 61404081) and the Shanghai Municipal Natural Science Foundation (Grant No. 14ZR1417700).

#249353 Received 2 Sep 2015; revised 13 Oct 2015; accepted 30 Oct 2015; published 4 Nov 2015